Journal of Petroleum & Environmental Biotechnology
ISSN: 2157-7463
OPEN ACCESS Freely available online
Research Article

Hydraulic Concentric Tubular Pumping System Simulation and Testing

Clemens Langbauer*, Petr Vita, Jax Gerald, Judmaier Daniel

Petroleum and Geothermal Energy Recovery, Montanuniversitaet Leoben, Austria

ABSTRACT

Conventional artificial lift systems are limited in their application by depth, borehole trajectory, and the produced media's chemistry. This publication presents a performance analysis of the concentric tubular pumping system, which combines the practical concentric tubular completion with the efficient reciprocating hydraulic piston pump to overcome the limitations of existing artificial lift systems cost-effective production for unloading of gas wells and heavy oil recovery. This pumping system consists of a specially designed plunger assembly and barrel combination driven by a hydraulic pressure unit from the surface without any mechanical connection. The hydraulic pump can be circulated into and out of the borehole or run by slick line, resulting in fast and low-cost installation. The pump is designed to run as a concentric tubular pumping system. This paper introduces the pump's concept, the fluid dynamics simulation, and pump testing at the pump test facility to prove its working principle. The simulations and lab tests have demonstrated very high system efficiencies. The lab tests confirmed the simulation results. At the defined pressure boundary conditions and a speed of 1.5 SPM, a production rate of 9.4 m^3/day at a lift efficiency of 95.4 percent was achieved. At 7.6 SPM, the production rate is 100 m^3/day, but the system efficiency dropped to 0.25. This pump's unique design requires a low number of moving parts, such as no mechanical connection to the surface and providing minimal exposure to wear and corrosion. Tests have shown that the pump is very adaptable regarding production rate, which requires a change in surface hydraulic pressure, which is typically in a range between 30 and 80 bars. Based on experience, the concentric tubular pumping system is the best selection for unloading gas wells to enhance the completions' lifetime. In This utterly new pump type exceeds the performance of existing artificial lift systems, increases the mean time between failures, and essentially reduces lifting costs.

Keywords: Hydraulic concentric tubular pumping system; Oil industry; Wax deposition

INTRODUCTION

A rising share of the conventional oil and gas fields and the trend towards green and emission reduced energy production push natural gas. The recovery of natural gas from conventional and unconventional gas reservoirs causes challenges for the operators. The removal of gas from the reservoir results in a drop of the reservoir pressure, a reduction of the drawdown, and a decline in the gas production rate [1]. As soon as the gas flow velocity in the production system drops below critical velocity [2,3], the gas well tends to load up with produced or condensed water or gas condensate. The accumulated liquid column causes a counter pressure against the reservoir, resulting in a fast drop or even stop of gas production.

Liquid loading of gas wells refers to the produced gas's inability to remove the wellbore's produced liquids. Liquid loading does not occur abruptly but is a gradual process. Early liquid loading detection is the key to prevent the well from dying. Typical symptoms are spikes, instantaneous tubing pressure changes, variable production rate, and sharp pressure gradients along the wellbore [3]. The industry applies several different methods to overcome the issue of liquid loading. These methods apply various physical and chemical methods to get rid of the accumulated liquid. Boundary conditions like the nature of the reservoir and the surface infrastructure are essential in selecting the most efficient method.

METHODOLOGY

Measures to maintain gas flow can be divided roughly into Type I and Type II methods [4]. Type I methods improve the liquid lift effectiveness based on the available reservoir pressure. Foam lifting uses surfactants inserted as soap sticks or batches into the wellbore and changes the surface tensional interaction between gas and liquid, thus adjusting the critical velocity. Foam lifting is the easiest and most economical way of deliquification for vertical wells [5]. Wellhead compression is applied to reduce the wellhead pressure below flow line pressure, enabling an increase

Correspondence to: Clemens Langbauer, Senior Researcher, Petroleum and Geothermal Energy Recovery, Montanuniversität Leoben, Austria, Tel: +4338424028204; E-mail: clemens.langbauer@unileoben.ac.at

Received: December 26, 2020, **Accepted:** February 01, 2021, **Published:** February 08, 2021

Citation: Langbauer C, Vita P, Gerald J, Judmaier D (2021) Hydraulic Concentric Tubular Pumping System Simulation and Testing. J Pet Environ Biotechnol. 9:416.

in the drawdown. A compressor is situated next to the wellhead to compress the gas from the wellhead into the flow line [6]. A flow velocity increase is achieved by a reduction of the flow cross-section and gas temperature maintenance. Small isolated tubing strings or coiled tubing strings are used [7]. These techniques are limited to a certain amount of water and moderate bottomhole pressure.

Type II methods are applied for wells with very low reservoir pressure, and significant energy needs to be added to the system by using artificial lift systems. Many artificial lift systems are in place to address gas-well deliquification under large quantity liquid removal. One needs to keep in mind that the installation of artificial lift systems is, in most situations, more expensive than one of the Type I methods. In general, Electric Submersible Pumps (ESP), Progressive Cavity Pumps (PCP), Sucker Rod Pumps (SRP), Hydraulic Piston Pumps (HPP), and Gas Lift Systems (GL) can be employed for moderate rate lifting in the oil field.

SRPs represent the major share of all globally installed units. The high system efficiency, based on the pump's principle and the flexible application range, is a significant advantage in terms of temperature, production rate, and pumped fluid composition. The rod string, which connects the surface unit with the downhole pump, is subjected to failure under certain conditions. ESPs represent the major share based on production rate. Different pump sizes allow the application of ESPs for a wide range of production rates. Complex downhole equipment, inability to handle gas, and high costs limit their applicability [8]. Although HPP, GL, and PCP have a relatively small market share, compared to ESPs and SRPs, their key attributes do not have to spare the comparison with other artificial lift systems. Table 1 compares the criteria gas handling capacity, maximum achievable drawdown, pump component temperature resistance, lift height, applicability in deviated wells, and hydraulically or by wireline accessibility. The attributes poor, fair, good, and excellent show the applicability for unloading gas wells.

SRPs are limited by the lift height and deviation of a well. ESPs have fair temperature resistance and cannot be retrieved hydraulically or by wireline. Gas lift systems cannot achieve a high drawdown, and PCPs are limited in lift depth, wellbore deviation, and temperature. Hydraulic piston pumps represent an alternative in this field of operation.

Standard hydraulic piston pumps have been successfully used to unload gas wells [9]. Several modifications of hydraulically powered downhole pumps for unloading gas wells have been designed and operated in the industry. A selection of these pumps and the performance are described in [4,10-12].

Heavy oil is classified as crude oil, having an API gravity lower than 20 and a low fraction of volatile constituents. Many high molecular weight constituents result in high fluid viscosity, a low recovery factor, when using conventional recovery techniques, and challenge artificial lift systems. Thermal and non-thermal recovery methods are used for heavy oil production [13]. Typical properties of heavy oil production are an oil gravity of 13° API, an oil viscosity between 100,000 cp at 20°C and 2,000 cp at 50°C, and production rates range between 30 to 50 m^3/day at moderate size casings, like 7 in [14].

Thermal heavy oil recovery methods are field-proven methods, where heat is induced into the reservoir layer to reduce the heavy oil viscosity. Steam-assisted gravity drainage is one form of steam flooding, where steam is injected into the upper of two well, positioned on top of each other, which relies on gravity drainage. The steam condensation in the reservoir increases the heavy oil temperature, resulting in a drop in the oil's viscosity, allowing its flow into the lower production wellbore [13].

Non-thermal heavy oil recovery methods are applied to thin reservoirs, where heat losses to surrounding layers make thermal oil recovery methods inefficient. Chemically enhanced oil recovery techniques, like alkali-surfactant flooding, are applied to increase the oil phase's mobility ratio [15]. CO_2 can dissolve effectively into heavy oil. CO_2 injection reduces the oil phase's viscosity in the reservoir [16]. Vapor-assisted petroleum extraction is a process where solvents are injected through one of two neighboring wells at low pressure into the reservoir to dilute the heavy oil [17].

Effective heavy oil recovery requires a large total contact area of the wells with the reservoir. Multilateral completions are state of the art, reducing the overall field development costs [18]. As heavy oil is commonly found in unconsolidated formations, sand control techniques, like gravel packs, screens, and downhole desanders, need to be installed.

Heavy oil production employs natural flow or mostly artificial lift systems. Several publications have presented an assessment for artificial lift systems. The wide range of heavy oil recovery methods requires splitting the assessment into two categories: lift methods suitable for thermal recovery and lift methods suitable for non-thermal recovery methods. Lifting systems for thermal recovery oil have to deal with low gravity, moderate viscous oil (up to 300 cp) at high temperature (up to 220°C). Lifting systems for non-thermal recovery have to deal with a mixture of high viscous oil and chemicals at low temperatures. Table 2 summarizes the performance evaluation of various artificial lift systems based on Worth, D. et al. [19].

Worth, D. et al. investigated SRPs, ESPs, and PCPs and ranked sucker rod pumps to be the best choice for pumping thermal and

Table 1: Performance of Type II methods for unloading of gas wells.

Variables	SRP	ESP	GL	PCP	HPP
Gas handling capacity	Poor	Poor	Excellent	Fair	Fair
Max. drawdown	Excellent	Fair	Poor	Excellent	Excellent
Temperature resistance	Excellent	Fair	Excellent	Poor	Excellent
Lift height	Poor	Good	Good	Poor	Excellent
Deviated wells	Poor	Good	Excellent	Poor	Excellent
Accessible (Hydraulically or by slickline)	No	No	Fair	No	Good

Table 2: Performance artificial lift systems for heavy oil recovery.

Variables	SRP	ESP	GL	PCP	HPP
High fluid viscosity	Good	Poor	Poor	Excellent	Good
Rate and head	Good	Fair	Good	Good	Good
High fluid temperature	Excellent	Poor	Excellent	Poor	Excellent
Deviated wells	Poor	Good	Excellent	Poor	Excellent
Solids	Fair	Fair	Excellent	Good	Fair

non-thermal recovery oil from vertical wells with the second choice on full metal housing PCPs. In inclined wells, metal housing PCPs are the preferred choice, as rod pumps tend to rod floating when pumping high viscous fluids.

Field observations of sucker rod pumps in thermal oil recovery wells have shown sand accumulations in the pump and excess surface load caused by increased fluid viscosity and rod string friction. In PCPs, galling effects have been seen due to the high temperature [20]. Another field study indicated failures at the rod string, like rod string buckling and corrosion, as the most significant share of sucker rod pump failures in heavy oil recovery. Rod string overloading and downhole pump failures have been seen as the most prominent issues when using PCPs [21].

New artificial lift system types have been developed and successfully field-tested for heavy oil recovery in the past. López Manríquez A, et al. [22] introduced a hybrid artificial lifting system, which is based on the injection of power fluid from the surface to the downhole positioned venturi tube. A solvent is used as a power fluid, which mixes with the heavy oil in the venturi tube and reduces the oil viscosity.

The Hydraulic Concentric Tubular Pumping System combines the advantages of a full metal design, which allows its application at any temperature, a rodless design to prevent friction and tubing wear, and the possibility of low-cost solvent injection. This new artificial lift system is ideal for the recovery of heavy oil and unloading mature gas wells.

CONCENTRIC TUBULAR PUMPING SYSTEM

This paper introduces a high-efficiency, low-cost hydraulic pumping system installed in a concentric tubular pumping system.

Concentric tubular completion

Conventional completions with more than one tubing string, so-called dual completions, require larger diameter wellbores, as the tubing strings are installed side by side (Figure 1). Dual completions are used when more than two independent connections into the wellbore are required. The conventional design comes along with several disadvantages. Large wellbore diameters cause higher drilling, casing, and cutting disposal costs. The installation of the side-by-side arrangement is a potential for failure. In case an isolated tubing is used to conserve the heat of the pumped fluid, the space limitation becomes even worse.

The concentric tubular completion is a pipe in the pipe system. The three flow paths are inside the smallest tubing, the annulus between the two tubing strings, and the annulus between outer tubing and casing. Figure 1 shows the equipment sizes of a comparable standard dual completion and a concentric tubular completion. The standard dual completion requires at least an 8 5/8" production casing string to provide enough space for the completion. The concentric tubular system consists of 2 7/8" inner tubing and a 5" outer tubing installed in a 7" production casing string. The flow cross-sections of the two inner sections are almost equal in size.

In summary, the advantages of the concentric tubular completion are:

- Tubing annulus cross-section is larger than the 2 7/8" tubing inner cross-section, resulting in beneficial lower flow velocities of the flowing fluid
- The installation procedure is less prone to failures and faster
- Smaller existing wellbores can be equipped with a concentric tubular completion than with a standard dual completion
- More economical and less environmental impact [23].

Standard hydraulic reciprocating piston pumps

A hydraulic reciprocating piston pump adds energy to the reservoir fluid to enable its flow to the surface, being actuated by pressurized power fluid. The high-pressure power fluid, generated at the surface, is injected via a separate flow path to the downhole pump. At the downhole pump, the power fluid drives the pump`s engine piston and returns either as a mixture with reservoir fluid in one tubing string (open system) or two separate tubing strings (closed system) to the surface [24].

The working principle of hydraulic piston pumps can be compared to that of sucker rod pumps because of the downhole pump's similar structural components, as check valves, pump plunger, and barrel are used. Typical single-acting systems only force fluid into the pump's discharge channel during the up- or the downstroke,

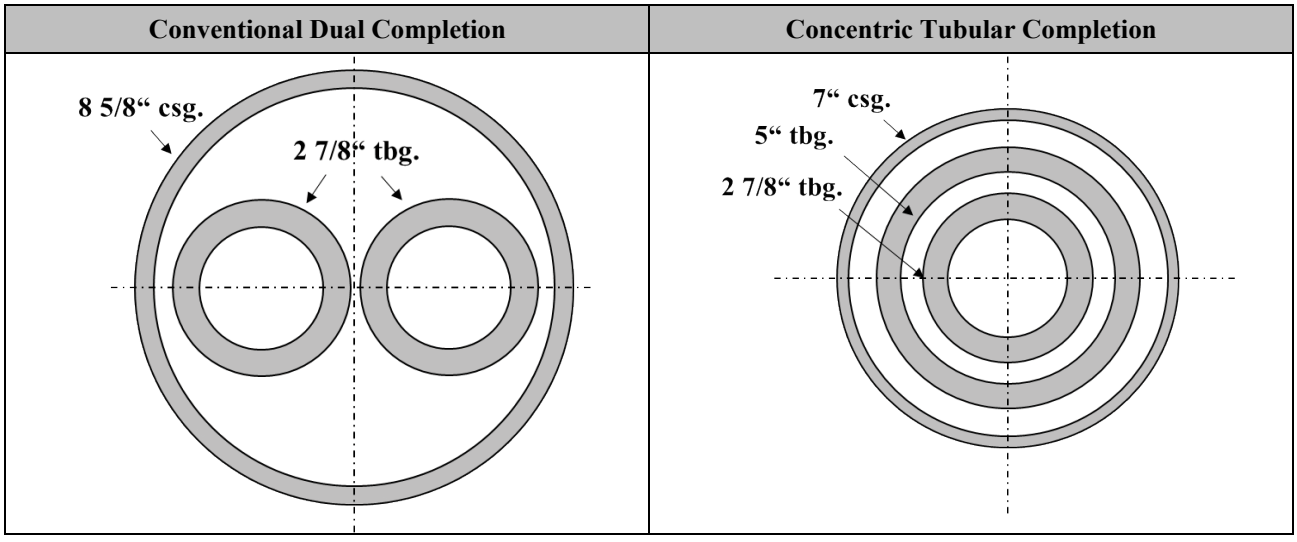

Figure 1: Size comparison between standard dual completion and concentric tubular completion.

whereas double-acting pumps can utilize both strokes for fluid displacement.

Standard hydraulic piston pumps' working principle is based on the reversing valve situated within the pump's engine piston. The reversing valve moves periodically up- and downward and is thereby opening and closing a pressure communication channel that directs the engine piston's lower or upper chamber's power fluid. The engine piston, which is directly connected to the pump piston, is forced upward, respectively downward. During the piston assembly's upstroke, low-pressure reservoir fluid is sucked through the pump chamber's intake valve. During the downstroke, the fluid in the pump chamber is displaced by the pump piston through the discharge valve into the high-pressure production tubing string. After that, the reversing valve switches again, and the next cycle is initiated. The ball and seat valves of the pump are opened and closed through changes in fluid pressure.

Existing hydraulic piston pumping systems have some limitations. Components control the pump piston's up- and downward motion, directly implemented in the subsurface pump, requiring additional moving components in the wellbore. Two parallel tubing strings are used-one for the injection of power fluid and another for producing the mixture of reservoir and power fluid. Conventional hydraulic piston pumps use almost the same amount of power fluid as produced reservoir fluid, resulting in significant flowing liquid quantities, causing a significant fluid frictional pressure drop.

Concentric tubular hydraulic pumping system

The concentric tubular hydraulic pumping system is a single-acting hydraulic pump type installed in a concentric tubular completion and is especially suitable for unloading gas wells and pumping heavy oil. For both applications, unloading gas wells and heavy oil recovery, the tubing annulus is used for reservoir fluid production and power fluid injection; the tubing – casing annulus is occupied by the gas flow. For unloading of gas wells, the inner tubing is filled with fluid to counterbalance the plunger movement, whereas for lifting heavy oil, solvents can be injected through the inner tubing.

The downhole structure of the presented pump type consists of a double plunger/barrel system, where the upper plunger is of larger diameter than the lower one. Plunger combinations like 2.75/2.25 in. or 2.25/2.00 in. can be chosen to define the pump's performance. A 1 in. diameter rod connects both plungers. This rod's length defines, besides the barrel lengths, the stroke length of the downhole pump (Figure 2) [25]. The assembly forms a constant volume but moving discharge chamber. Next to the rod, a pre-drilled section allows communication with the tubing annulus. At the end of the lower plunger, a traveling valve is located. Below the lower plunger, the pump's intake chamber, whose size is changing during the stroke. At the bottom of the lower barrel, the standing valve is in place. The third ball/seat valve is located at the end of the concentric tubular completion.

The working principle of the presented hydraulic piston pump is straightforward. The inner tubing string is entirely or partially filled with inhibited liquid, where the level depends on the plunger sizes and the requested pump performance. The tubing annulus is filled with a mixture of the discharged reservoir fluid and power fluid. For power fluid treated reservoir fluid is selected. A directional valve at the surface connects the tubing annulus alternating to the flow line during the plungers' downstroke or high-pressure power fluid during the plungers' upstroke. To initialize the plungers' upward movement, the directional valve connects the power fluid line to the tubing annulus and disconnects the flow line. High pressure is acting on the plunger ring area, the large plunger cross-section minus the small plunger cross-section, and is pushing the plunger upwards. As a result, reservoir fluid is sucked through the two standing valves into the downhole pump's enlarging intake chamber, whereas the traveling valve is closed. When the directional valve switches and disconnects the power fluid line, the tubing annulus pressure drops, and the plunger assembly is pushed downwards by the hydrostatic weight of the liquid in the inner tubing string. Simultaneously, the reservoir fluid in the intake chamber is discharged through the hollow lower plunger into the tubing annulus and produced. The large plunger has no bore and is closed. The power fluid's pressure magnitudes and the flow line, and the tubing's liquid level define the plungers' motion characteristics [26].

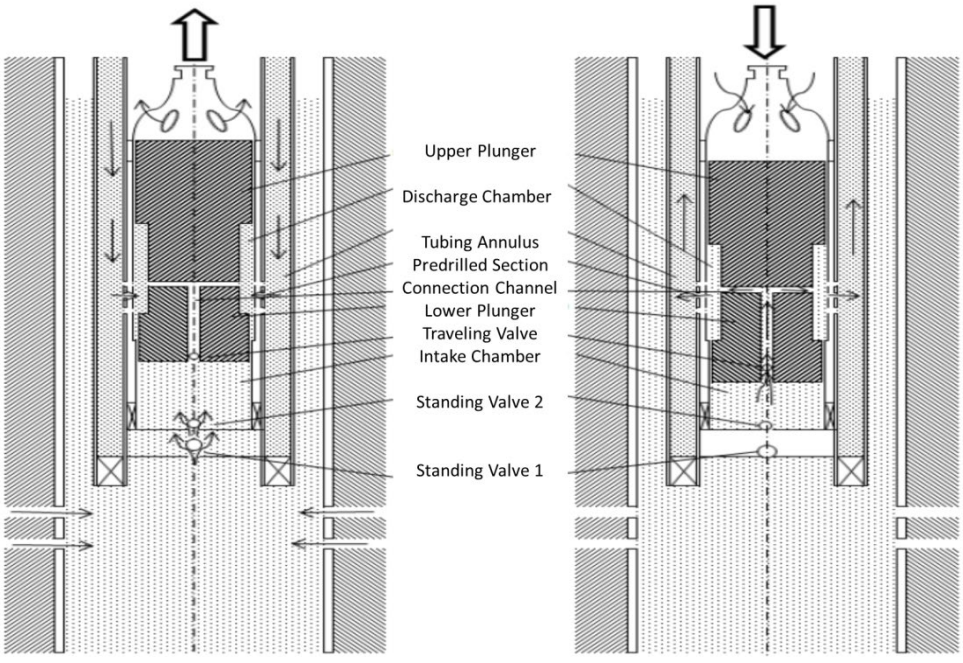

Figure 2: Schematic drawing of the hydraulic pumping system.

The pump capacity depends on the smaller plunger size and the stroke length. The upper plunger size and the fluid level in the tubing result in the power fluid pressure. A high rate of production requires a large lower plunger size. For operation mode one, a partially filled tubing string is required. The fluid level needs to be monitored as it influences the production characteristics of the pump. The annulus's liquid level change can be done by installing a spring-loaded check valve and a bore at the downhole pump's upper plunger. By applying a gas pressure at the tubing wellhead, liquid from the inner tubing is replaced into the pump's discharge chamber. In the same way, for example, an inhibitor can be dosed into the downhole pump. In contrast, a moderate-sized upper plunger and a filled tubing string can achieve low rate fluid production.

The pumping system is designed to lift fluid for low intake pressure situations. The pump can be used to reduce the bottom hole pressure of a wellbore to its minimum. As a result, the simulation and the lab tests have to prove the pump's working principle at low intake pressures.

System installation

The system's installation starts with running in the first tubing of the concentric tubular completion with the bottom's standing valve, required for closed-loop fluid circulation. The second step depends on the pump size. Small pump sizes can be circulated into the wellbore, whereas large systems need to be run as part of the inner tubing string. In case the pumping system can be circulated in, the next step is installing the inner tubing string, with the pre-drilled section, a packing element to seal against the larger tubing, and the landing nipple for the pump. Afterward, the workover fluid in the inner tubing is replaced by inhibited fluid, and finally, the downhole pump is circulated in and fixed in the landing nipple. Figure 3 illustrates the procedure, where a 1.75/1.5 in pump is installed [27].

1st step (a): Run in the outer tubing, including the standing valve at the bottom, and hang off in the wellhead tubing hanger.

2nd step (b): Run in the inner tubing with a pre-drilled section at the bottom, including the landing nipple for the hydraulic pump. Hang the tubing string in the wellhead tubing hanger and seal at the bottom against the outer tubing.

3rd step (c): Replace workover fluid with power fluid

4th step (d): Run in and fix the hydraulic pump in the landing nipple.

To mitigate gas or sand production through the pump, conventional sucker rod pump equipment can be used. Downhole gas separators or downhole desander [28] are available.

SURFACE FACILITIES

The surface facilities are the wells' essential elements, equipped with a hydraulic pumping system [29]. Surface facilities are regularly seen as a crucial point due to their often-high footprint on the ground level. Pressure vessels, multiplex positive displacement pumps, separators, and additional equipment are needed. Nonetheless, the overall high footprint can be reduced or seen as less problematic if several wells share the surface facilities at onshore clusters or offshore platforms.

At the surface facilities, multiplex positive displacement pumps typically provide the high-pressure power fluid for the downhole pump. Alternatively, multistage centrifugal pumps could be used,

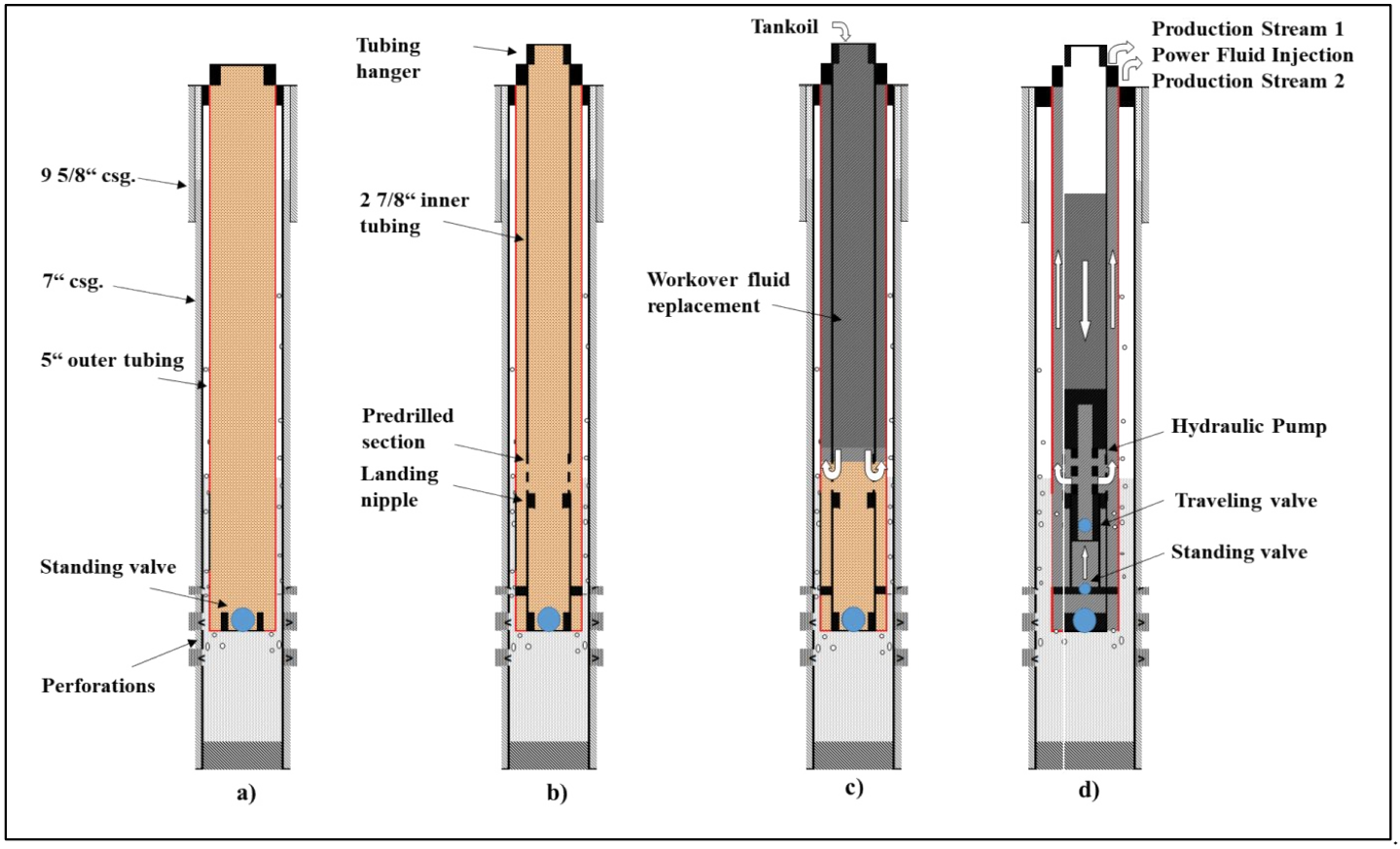

Figure 3: Hydraulic concentric tubular pumping system installation procedure for small pump sizes.

but it is rarely a viable option due to efficiency issues. The pumps are usually driven at 200-450 rotations per minute to reduce vibrations, noise emissions and prevent fluid oscillation problems. Pulsation dampeners are installed downstream of the pump to reduce the effect of pulsating flow. These dampers can also detain pipe vibrations and lower the load on the pump itself [30]. In cluster solutions, a control manifold is installed to distribute the power fluid to each well. At the wellhead of a hydraulic pumping system, a wellhead control valve or a four-way valve is installed, switched to different modes. A switch of this valve causes reverse circulation, which circulates the pump out of the wellbore. Moreover, a pressure gauge and a constant-pressure controller are installed. A separator is installed for the separation of reservoir fluid, power fluid, and gas. To clean the power fluid before injection, a power fluid treating facility must remove abrasive materials as solids.

The complexity and the footprint of the presented system's surface facilities are smaller compared to standard systems. During the plungers' upstroke, reservoir fluid is pushed into the tubing annulus to the surface (Figure 4). Directional valve 1 directs the fluid into the flow line that is connected with the separator.

In the separator, volatile or lightweight liquids are separated and forwarded into the flow line. Close to the bottom, the fluid, which is used as power fluid, is taken. The power fluid is compressed into a high-pressure tank by the continuously operating positive displacement pump. The high-pressure tank is connected to directional valve 1-the directional valve 1 switches to change downhole pump direction into downstroke. The separator's connection is blocked, and the high-pressure tank's power fluid is pushed into the tubing annulus. Directional valve 2 is used to keep the liquid level in the inner tubing by pumping a defined amount of power fluid, constant for high rate fluid production.

Testing and optimizing new systems is time-intensive and costly. A detailed analysis of the downhole pump has been performed before testing in the lab to reduce the number of uncertainties and speed up the development process.

PUMP PERFORMANCE SIMULATION

A computational fluid dynamics simulation (CFD) was performed to evaluate the planned design and the hydraulic concentric tubular pumping system's performance. The objectives are to investigate the plunger movement characteristics and potential drawbacks because of extraordinary high velocities, which might cause erosion of the pump's plungers.

Force balance at the plunger

The basis for the CFD simulation is a detailed force analysis at the plunger. It considers the changing pressures, plunger weight, friction forces, and fluid weight in the inherent tubing system. A closer investigation identified five forces interacting with each other. The schematic in Figure 5 indicates the relevant forces.

Where m_{it} is the fluid mass in inner tubing, m_{ta} is the fluid mass in tubing annulus, and m_p is the weight of the plunger. A_{it} is the cross-sectional area of the discharge chamber, A_{ich} is the cross-sectional area of the intake chamber, and A_{eff} is the effective cross-sectional area and equal to A_{it}-A_{ich}. The pump cycle is controlled by manipulating the tubing annulus pressure p_{ta} acting on the reciprocating piston's effective cross-section through the power fluid and resulting in the pressure force $F_{p,ta}$. It is acting against

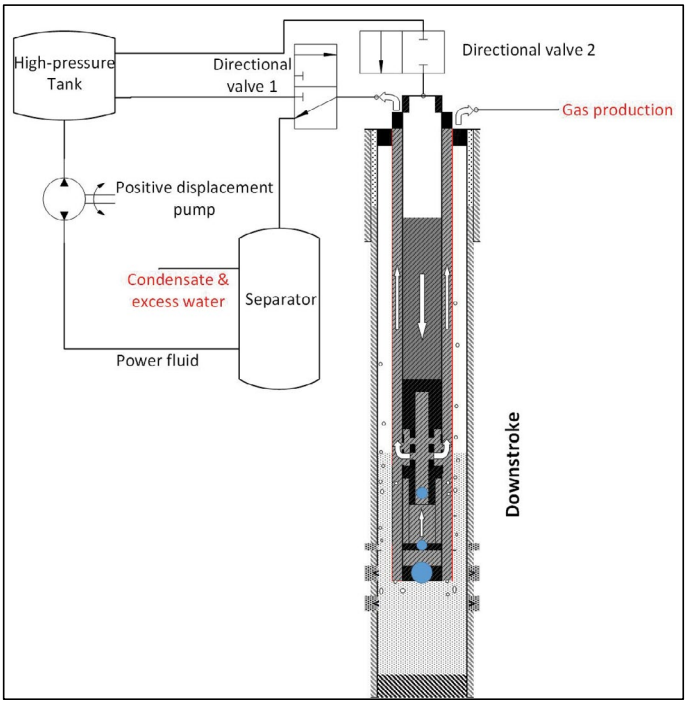

Figure 4: Surface facilities schematics.

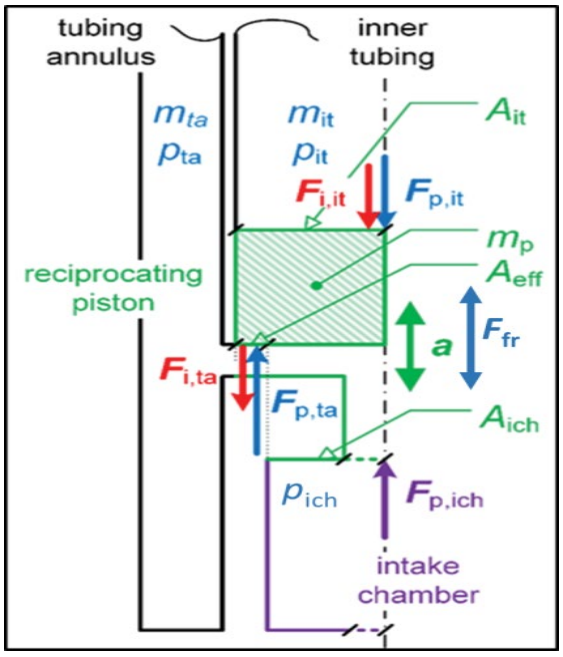

Figure 5: Forces acting on the piston [26].

the pressure force $F_{p,it}$ in the tubing, applied on the upper plunger cross-section because of the fluid pressure pit in the inner tubing. The intake chamber force $F_{p,ich}$ is the result of the intake pressure p_{ich}, provided by the reservoir and the lower plunger's cross-section. F_{fr} represents the mechanical friction between the plunger and the barrel.

Once the plunger starts the movement, additional inertial forces act on them. The most prominent ones are the inertial force $F_{i,it}$ of the fluid in the inner tubing, and the fluid inertial force $F_{i,ta}$ referencing to the fluid in the tubing annulus. Both are acting against the motion of the plunger.

D'Alembert's principle states that if all forces acting on a body do not balance, the body starts to accelerate. A force imbalance at the downhole pump's plunger results in a movement, which can be

controlled by combining the tubing and tubing annulus' pressure magnitudes. Eq. 1 shows the force balance at the pump plunger, where a is the plunger acceleration.

$$a = \frac{\sum_k F_k}{\sum_l m_l} = \frac{\left(F_{p,ta} + F_{p,ich} - F_{p,it} - F_{fr} - F_g\right)}{\left[m_p + c_{a,ti}.m_{it} + c_{a,ta}.m_{ta}\right]} \quad (1)$$

The parameters $c_{a,ta}$ and $c_{a,ti}$ represent correction factors for the inertial forces because the fluids are flowing in different cross-sections; thus, different fluid accelerations occur. The plunger acceleration can be converted to velocity and displacement s, which is limited by the pump's stroke length l_s.

$$s = s_0 + v_0 \Delta t + \frac{1}{2} a \Delta t^2 \quad (2)$$

Where v_0 and s_0 represent the initial piston velocity and displacement, Δt is the time increment. The theoretical pumped volume per stroke q_{th} is given by the discharge chamber volume (Eq. 3).

$$q_{th} = A_{it} l_s \quad (3)$$

The output work W_{out} of the pump is given by the effective production rate and the injected quantity of power fluid times the discharge pressure p_d at the surface (Eq. 4).

$$W_{out} = \eta_{vol} q_{th} p_d t_{downstroke} \quad (4)$$

Where η_{vol} is the pump volumetric efficiency, $t_{downstroke}$ is the duration of the downstroke, and p_d the discharge pressure of the wellhead. The invested work W_{in} into the pumping system is equivalent to the volume of fluid injected at the wellhead, times injection pressure p_{inj}, and the duration of the upstroke $t_{upstroke}$.

$$W_{in} = \left(A_{it} - A_{ich}\right) p_{inj} t_{upstroke} \quad (5)$$

The system efficiency is the output work divided by the invested work.

Computational grid

Based on the downhole pump geometry, an axisymmetric computational model was derived. The chosen way to create the mesh for this numerical study is the blockMesh utility of OpenFOAM [31] because of its possibility of mesh parameterization. The configuration file blockMeshDict contains all the geometry vertices, further specified into blocks (Figure 6). After defining the blocks, the mesh is further refined at the most relevant zones to better resolve the flow behavior. As the last step within the blockMeshDict, all faces of the structure are defined.

Arbitrary Coupled Mesh Interface

One of the critical features mandatory for the model's set-up is the fluid flow connection between the tubing and the pump assembly. OpenFOAM can apply an Arbitrary Coupled Mesh Interface (ACMI), more commonly known as Sliding Interface, for such dynamic mesh cases. Before creating the baffles in the file create BafflesDict to make the ACMI working, so-called "faceSets" and "faceZoneSets" are defined for different mesh regions within the configuration file topoSetDict. With the pump plunger's movement, the barrel volume changes, which must be implemented in the model. Therefore, a deformable mesh region (Figure 6) that reacts to the pump's movement must be created. To achieve that, the file dynamicMeshDict is configured for a mesh motion solver displacement Layered Motion and the active mesh regions.

Solver

OpenFOAM's solver pimpleDyMFoam realizes the discretization of the equation system and its implementation. The solver *pimpleDyMFoam* supports the dynamic mesh movement [32,33] needed to model the reciprocating plunger and the intake chamber in the simulation. To validate the hydraulic subsurface pump concept, a simulation model using the open-source software toolbox OpenFOAM® and its supporting library swak4Foam [34] is set up.

Governing equations

The fundamental equations for the incompressible fluid flow model are the continuity equation (Eq. 6) and the momentum equation (Eq. 7). The assumption of incompressibility enables removing the density ρ from the equations, which leads to a simplification of the system. With constant density, the energy equation can be solved

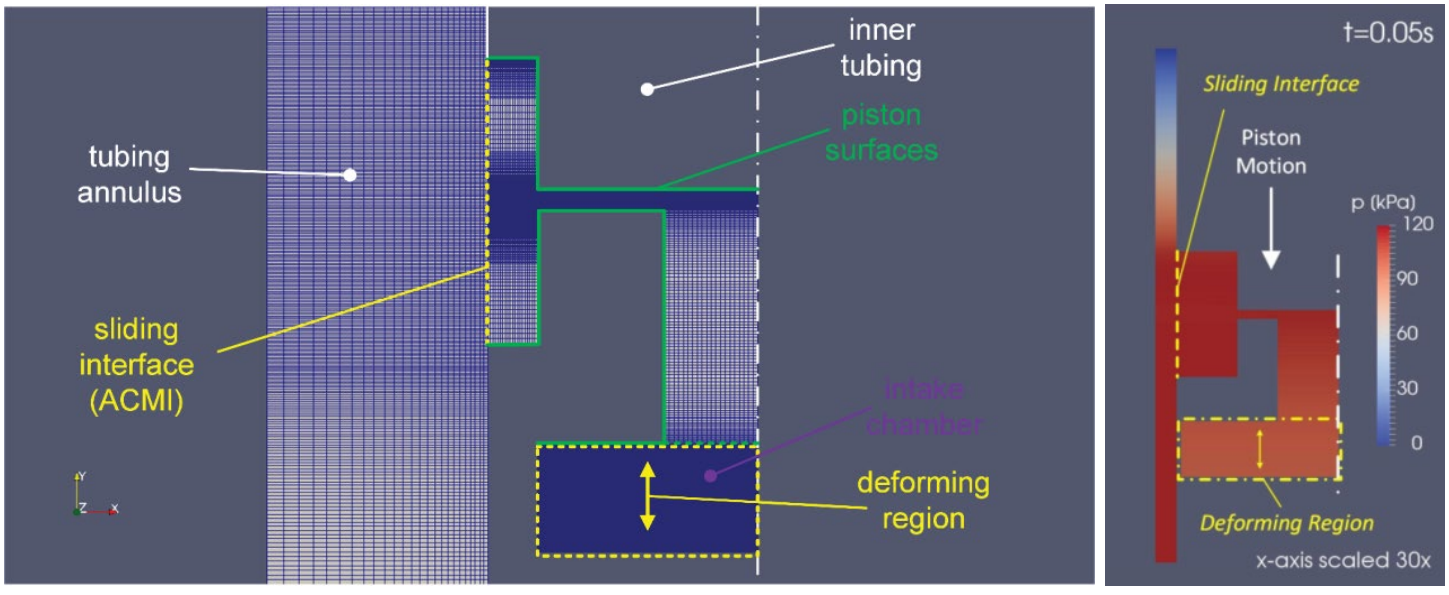

Figure 6: Computational grid detail (x-axis scaled 30x).

afterward [35].

$$\nabla . u = 0 \quad (6)$$

$$\frac{\partial u}{\partial t} + \nabla.(uu) = -\nabla P + \nabla.\left\{(\nu + \nu_t)\left[(\nabla u + (\nabla u)^T\right]\right\} \quad (7)$$

Where u represents the fluid velocity, P is the kinematic pressure, ν and ν_t are kinematic viscosity and kinematic turbulent viscosity, respectively, and t denotes time. The turbulence model supplies the kinematic turbulent viscosity. The selected turbulence model is the two-equation k-ω Shear-Stress Transport (SST) by F. R. Menter [36] for Reynolds averaged simulation (RAS). The k-ω SST model is a low-Re turbulence model and can describe laminar to turbulent flow transition within the pump.

SIMULATION RESULTS

The pump performance analysis was performed for two different scenarios: low rate production and high rate production. Plunger friction, pressure losses, and slippage at the plunger are considered for evaluating the hydraulic pump's performance, set a 1000 m deep in a vertical well. The liquid density is 1030 kg/m³, the flow line pressure is fixed to 6 bar, and the pump intake pressure is 2 bar.

Low rate production

Low rate production considers production rates up to 50m³/day, ideal for the unloading of gas wells. The analyzed downhole pump consists of a moderate-sized upper plunger, e.g., 2.50 inches, and a small size lower plunger, e.g., 1.50 inches. The stroke length can vary from 1 m to up to 8 m, directly influencing the flow rate. For comparison reasons, a stroke length of 3.75 m was selected. The concentric completion consists of a 3 ½" inner tubing and a 5 ½" outer tubing. The inner tubing size allows the circulation of the downhole pump without a workover rig. The inner tubing is filled with fluid, but it's wellhead pressure is set to zero.

The static equilibrium pressure at the surface, provided by the power fluid buffer tank, is 55.7 bar for the selected geometry. To lift the plunger, a higher pressure must be applied to let the plunger drop, resulting in fluid production; the tubing annulus pressure is lowered below this equilibrium pressure. Two different operation modes are viable. A constant alternating pressure amplitude around the equilibrium pressure is representing Mode 1. Mode 2 shows a particular pressure increase during the upstroke and the entire pressure reduction to flow line pressure during the downstroke. Figure 7 shows the pressure boundary condition for both modes and a speed of 3 SPM.

Mode 1 results in equal up- and downstroke durations and a symmetric behavior between up- and downstroke. Mode 2 shows significantly faster downstroke velocities, resulting in shorter downstroke duration and a higher total production rate.

Figure 8 presents the characteristics of Mode 1. A minimum pressure amplitude of 6.5 bar has to be applied to initiate the system's movement, resulting in 1.25 strokes per minute, 0.93 kW power consumption, and a production rate of 7.23 m³/day. An increase in the pressure amplitude causes an increase in SPM and results, for instance, at 20 bar in 7.24 SPM and 41.9 m³/day fluid production. A power of 6.7 kW is thereby required.

High rate production

High rate production considers production rates from 30 m³/day up to 110 m³/day. The downhole pump consists of a moderate to a large upper plunger, e.g., 2.50 in, and a moderate size lower plunger, e.g., 2.25 in. The stroke length can vary from 1m to up to 6m, directly influencing the flow rate. For comparison reasons, a stroke length of 3.75 m is selected. The concentric completion consists of a 3 ½" inner tubing and a 5 ½" outer tubing. The tubing is partially filled with fluid, and the fluid level is used to regulate the strokes per minute, thus the pump's production rate. The boundary conditions are the same as for the low rate production situation to enable a comparison. The ratio between produced reservoir fluid to injected power fluid is for the selected pump plunger combination 4.0. For evaluating the average surface power requirements, the strokes per minute (SPM), the production rate, and the system efficiency are evaluated. The surface compressor compresses power fluid into the pressure accumulator during the whole cycle, but power fluid is just required during the plunger assembly's upstroke. In that sense, the average surface power is presented in Figure 10.

It can be seen that a liquid level of 760 m causes a low production rate of just 11.7 m³/day, but at a very high efficiency of about 93%. Deeper liquid levels do not operate the downhole pump. The shallower the liquid level, the faster the pump is operated, but the efficiency goes down. At a production rate of 114 m³/day, the efficiency is just 20%. Each upstroke requires 2.32 l of power fluid injected; thus, depending on the stroke per minute, the power fluid pressure tank volume must be selected. Typically, a volume of 50 l is enough. As a result, the pressure tank can be of moderate volume. The speed of the system can be adjusted by a change of the liquid level in the tubing.

Figure 11 shows the effect of the stroke length on the system's production rate and speed. The values presented are evaluated for

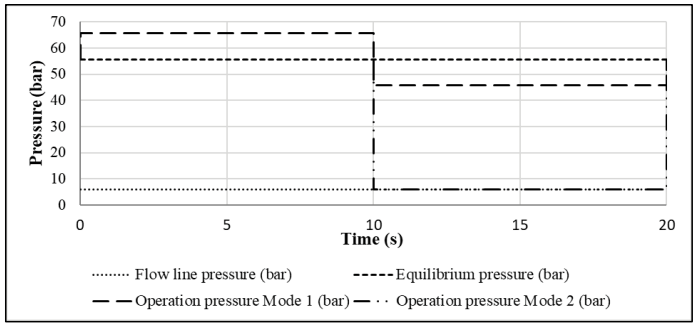

Figure 7: Low rate production–Pressure boundaries.

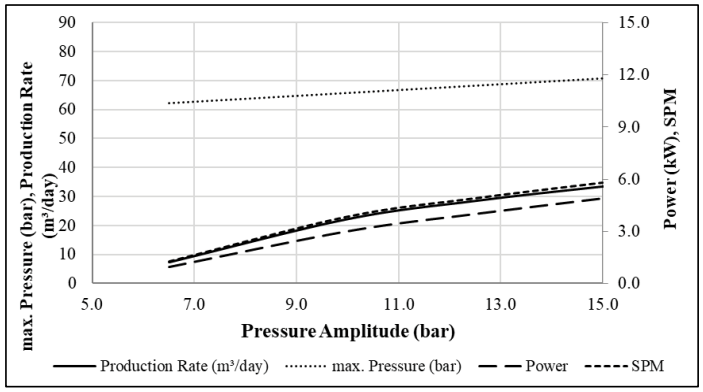

Figure 8: System behavior–Low rate production-Mode 1.

similar boundary conditions and show the same system efficiency. The longer the pumping system's stroke length, the lower the speed, which is beneficial concerning pump wear, and the higher the production rate.

The CFD simulation also allows the evaluation of the flow field and the pumped fluid pressure distribution. The pressure distribution in the pump's intake chamber for high rate production, with the fluid level at 720 m in the inner tubing, is shown in Figure 6. The plot shows relative pressures to the discharge pressure of the downhole pump. It can be seen that the fluid pressure increases slightly in the flow channel through the lower plunger and the bores through the barrel into the tubing annulus, which is the result of the cross-section decrease in this region. Figure 12 shows the pump's fluid velocity distribution with its velocity magnitude at two, respectively, three seconds. The plunger velocity at two seconds is 0.73 m/s, respectively 1.1 m/s for three seconds. After two seconds, the displacement on the left situation is 0.73 m, whereas, after three seconds, the plunger reaches 1.64 m. The highest velocity can be seen at the intake valve of the intake chamber. In the pump's flow channels, the simulation showed moderate velocities, and there is not an expectation of severe wear issue when pumping solids [37].

The inlet velocity of the reservoir fluid into the intake chamber during the pump's upstroke is plotted in Figure 13. As expected, it is increasing with time due to the accelerating motion of the piston. Maximum velocities of almost 4 m/s have been seen in the simulation results. A wear-resistant intake chamber valve will be used. Interesting thereby is the behavior at around one second and at 4.5 seconds that may result from the system's dynamics.

LARGE SCALE LAB TESTING

Intensive lab testing was performed at a pump test facility to verify the simulated behavior of the pump. The sucker rod pump module (see Figure 14) of the pump test facility, which was used for the tests, consists of three main elements: the housing of the downhole components, which is an 8 m long stainless steel casing of 6 5/8 in., a polished rod, and a linear drive. The housing enables operating pressures up to 40 bar at the temperature range from zero degree Celsius up to 60 °C. These conditions represent lift situations in the field, having a net lift of about 500 m. The linear drive is installed on top of the housing, allowing stroke lengths of 2 m and lift forces of 15 kN. The intake pressure can range from 2-10 bars at a flow rate of up to 100 m³/day. State-of-the-art instrumentation is installed on all components. Pressures, temperatures, vibrations, flow rates, and electricity consumption are just a selection of all recorded data. All data are processed by a logic controller and stored at the data server, using state-of-the-art software [38]. In the past, the pump test facility has already been used to develop new technologies for the industry [39].

Test setup

The tested prototype has a 2.75/2.25 inches plunger and a stroke length of 1.75 m (Figure 15). The pump is made of standard sucker rod pump equipment, which keeps the pump cost very low. The lower plunger is equipped with a 225 traveling valve. At the bottom of the lower barrel, the standing valve 2 of size 250 is situated. The tubing connector is used to connect the pump to the test facility's housing on top of the upper barrel.

The pump design is slightly adapted to the capabilities of the test

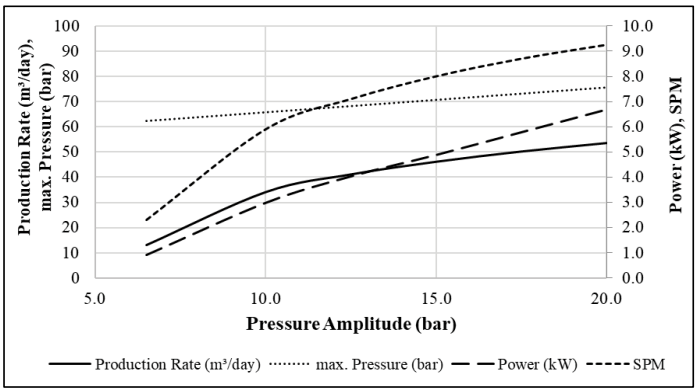

Figure 9: System behavior-Low rate production-Mode 2.

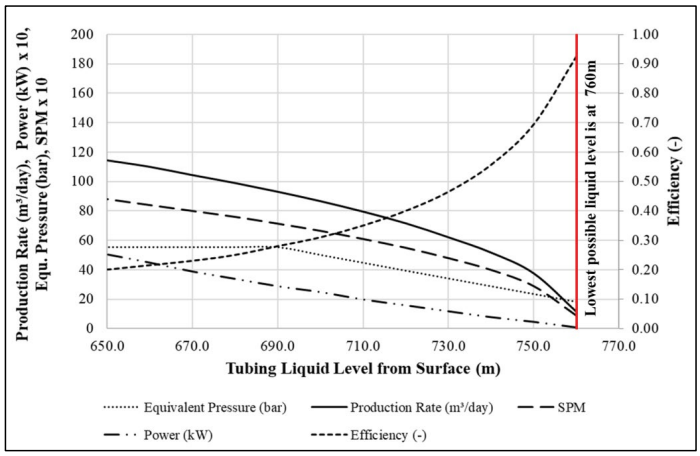

Figure 10: System performance–High rate production.

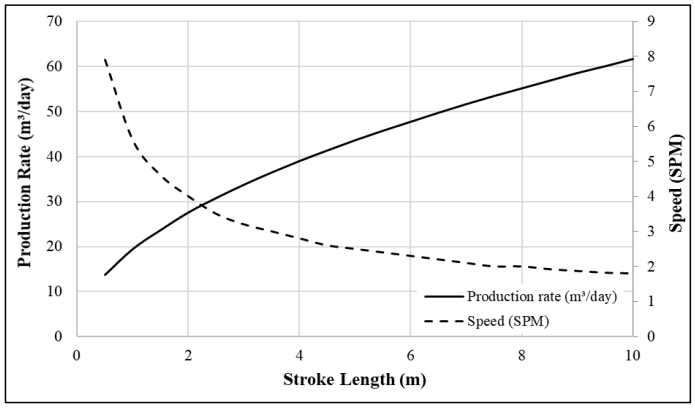

Figure 11: Effect of the stroke length.

facility testing (Figure 16). A rod is connected to the upper end of the larger piston and passes through the facility's top flange to enable the piston's simple position measurement. In a depth of four meters, the housing of the facility is split and connected by flanges. A sealing flange is installed at that position to divide the pump's intake section from the pump's discharge section. The barrel atop of the sealing flange is perforated, allowing communication of the pump plunger area to the pump discharge. The casing–tubing annulus is not part of the lab test.

Three pressure sources are required for running the tests. A low-pressure source representing the intake pressure, a back-pressure source representing the pumped fluid's flowline pressure, and a power fluid pressure source are used. Three pumps, two pressure vessels, and two atmospheric pressure tanks are used (Figure 17). An air compressor charges the fluid in the medium pressure storage

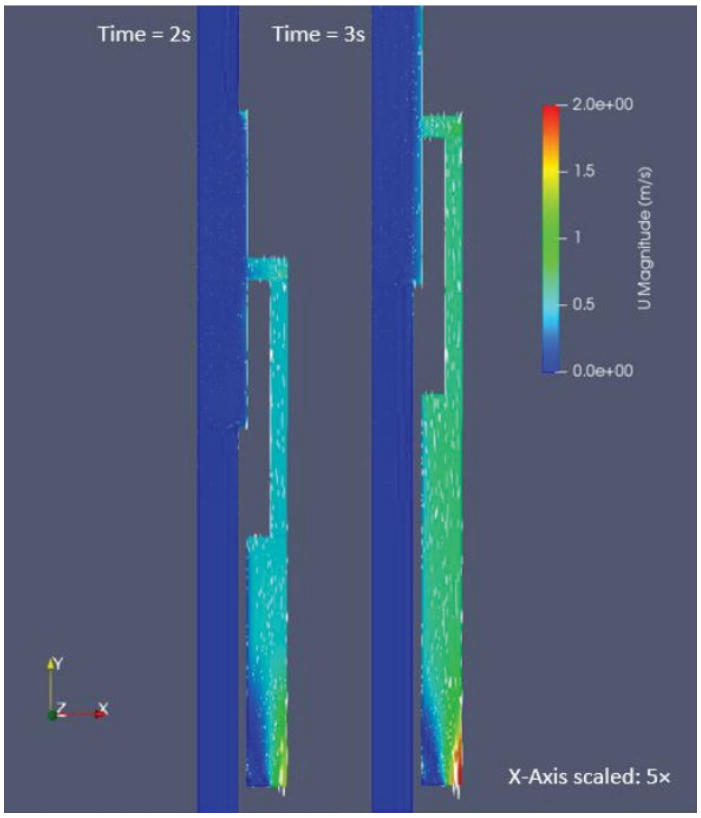

Figure 12: Velocity distribution in the pump for 5.5 strokes per minute [37].

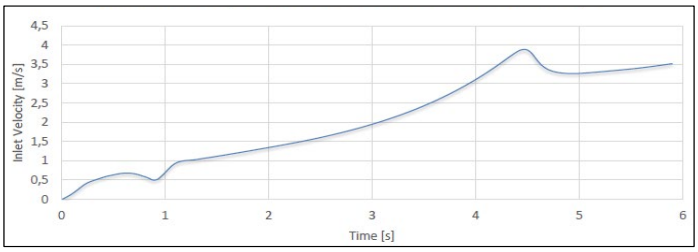

Figure 13: Inlet velocity distribution during the upstroke for 5.5 strokes per minute [37].

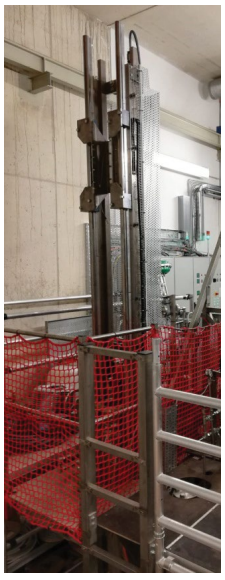

Figure 14: Pump test facility.

tank (D101_A) and provides pressure to the inner tubing string. A pressure sensor (D05_A) measures the actual pressure in the tubing. The medium pressure storage tank also provides the power fluid pump with fluid. The power fluid pump increases the fluid pressure (D04_A) and forwards the power fluid into the buffer to balance the power fluid consumption fluctuations. The fluid, entering the system through the downhole pump's intake, is taken from the atmospheric pressure storage tank, compressed by the intake pump, and sent to the bottom of the facility's housing. The pressure sensor D03_A records the intake pressure. The position sensor WE01_A is recording the position of the plungers.

Two valves are used to switch between power fluid injection, causing the downhole pump to move upwards and the fluid production, causing the pump to move downwards after the top dead point is reached. The produced fluid is directed into the atmospheric produced fluid tank to measure the produced fluid quantity. The force sensor KR03_A measures the produced fluid's gravitational force in the produced fluid tank, which allows the evaluation of the produced volume. Afterward, it is directed back into the atmospheric pressure storage tank.

Test execution and results

Four different scenarios have been tested at the Pump Test Facility. For each scenario, the inner tubing pressure was set to about 10 bar. The intake chamber pressure was defined to be 2.5 bar for test case 3, 4 bar for test case 3, and 6 bar for test case 1. Tests one to three were performed with the tubing full of water, whereas for test four, the tubing was filled with compressed air. The pumped fluid was fresh water at ambient temperature.

In test case 1, the constant intake pressure of six bar was applied to the system. The pre-set inner tubing pressure is 10 bar. Figure

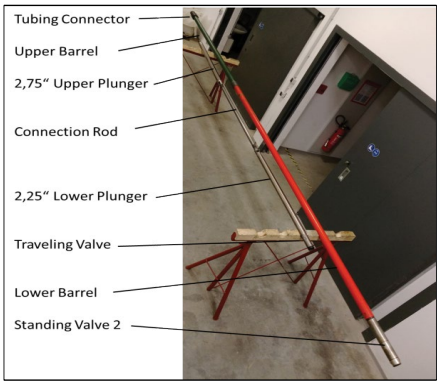

Figure 15: 2.75/2.25 inches × 1.5 m hydraulic pump prototype.

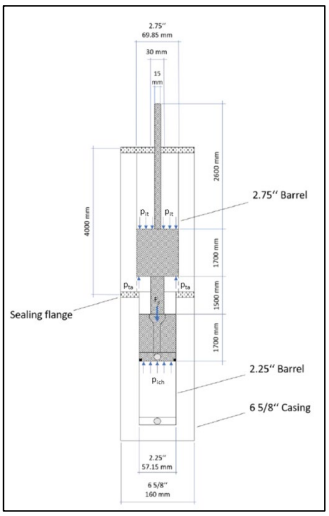

Figure 16: Pump setup for testing.

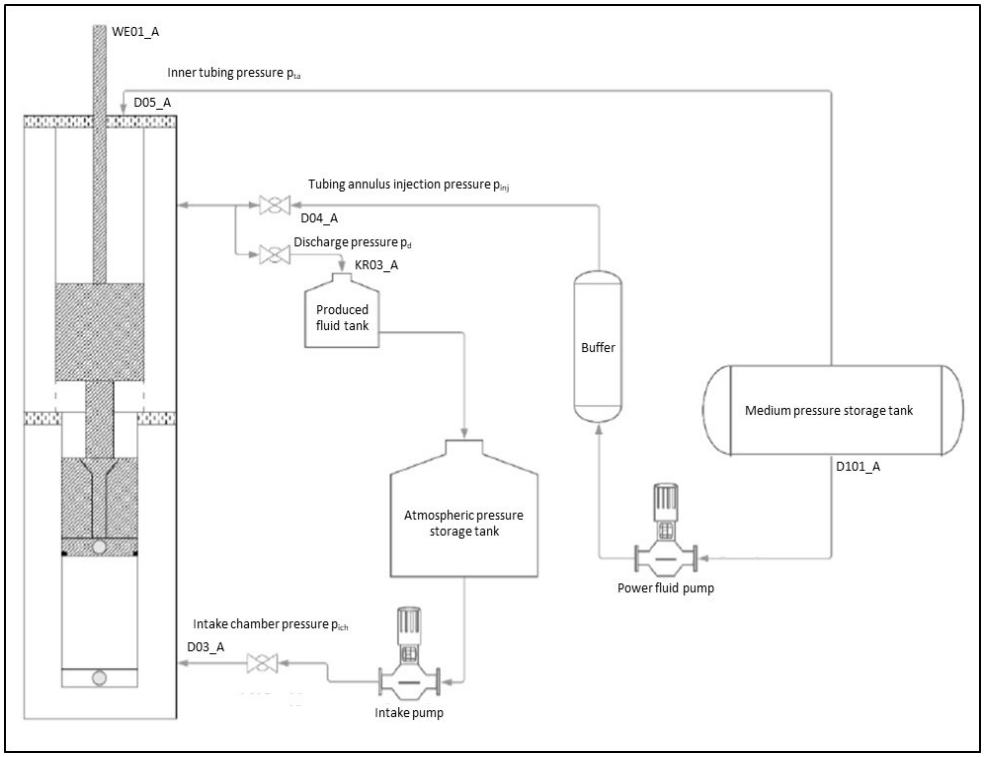

Figure 17: Testing schematic.

18 indicates that this inner tubing pressure dropped during the pump's downstroke because of the testing arrangement, where a pressurized tank applied the head pressure. There would not be a pressure drop in the field, as there is a fluid column on top of the upper plunger. The annular tubing pressure was alternated between the constant flow line pressure of about 8 bar and injection pressure. The injection pressure was changed throughout the test to vary the plunger velocity. The injection pressure magnitude can influence the upstroke duration, whereas the inner tubing pressure, the intake pressure, and the flow line pressure define the downstroke duration. The tested speed range was between 1.23 and 3.75 strokes per minute, reached by injection pressure changes. The injection pressure varied between 23 and 36 bar. The higher the injection pressure, the higher the upstroke velocity.

At the beginning of this test case scenario, various up- and downstroke profiles were tested at a low speed of about 1.5 strokes per minute. The upper diagram in Figure 18 presents the position, velocity, and acceleration of the plungers. The asymmetric stroke profile for the first five strokes can be seen. It shows a lower velocity during the second half of the upstroke. In test case 1, the maximum plunger velocity varied between 0.1 and 0.33 m/s. The plunger acceleration varied between 0.1 and 0.2 m/s^2. Viscous friction and inertia effects have been insignificant for the low strokes per minute cycles. The resulting forces on the plunger, calculated by the previously shown equations, are close to zero (Figure 18). For higher speed, imbalances due to dynamic effects can be seen.

For test cases, two and three similar observations were seen. The theoretical production rate of reservoir fluid per stroke for the stroke length of 1.75 m is 4.43 liters, whereas the required power fluid volume is 1.89 liters. The rate measurement of the produced fluid per stroke was about 5.9 liters, representing the injected power fluid volume and the produced reservoir fluid. The volumetric efficiency was between 90 and 96 percent for low SPM with a slightly decreasing trend (Figure 19).

The pump's total efficiency can be evaluated by comparing the work to be performed by the pump with the work to be invested into the system per stroke. The performed work of the pump is equal to the production rate times the discharge pressure. The invested work is equal to the injection rate time, the injection pressure, plus the intake pressure times intake rate. The total efficiency reaches values close to one at a low number of strokes per minute (Figure 20). With increasing SPM, the efficiency drops. At 3.5 SPM, the overall efficiency for the defined setup has dropped to about 50 percent.

The results of test case 4 are slightly different. The inner tubing pressure was set to 4.5 bar, and the intake pressure was set to 3 bar. These settings allowed a pump speed of almost 4 strokes per minute. The injection pressure was defined by 30 bar. In contrast to the other test cases, compressed air was provided by the pressurized tank. During the plungers' upstroke, the air was further compressed up to 10 bar, where the pressure was equalized during a hold period at the upper dead center with the pressurized tank. The motion profile looks similar to test cases one to three. The resulting force shows a higher imbalance due to the higher chosen SPM.

The green dots in Figure 20 indicate a total efficiency as low as 25 percent, which results from the air in the inner tubing being compressed and released during the upstroke of the plungers.

Figure 21 shows the results of case 4 in terms of motion, pressures, and force. The upstroke is faster since no water is needed to be displaced. The lower tubing head pressure causes a slower downstroke.

The test results have been compared to the simulation. The pressure limitations of the test facility required a downscaling of the simulated pump depth. The comparison is performed for a 100 m deep wellbore. The inner tubing is filled with fluid, and

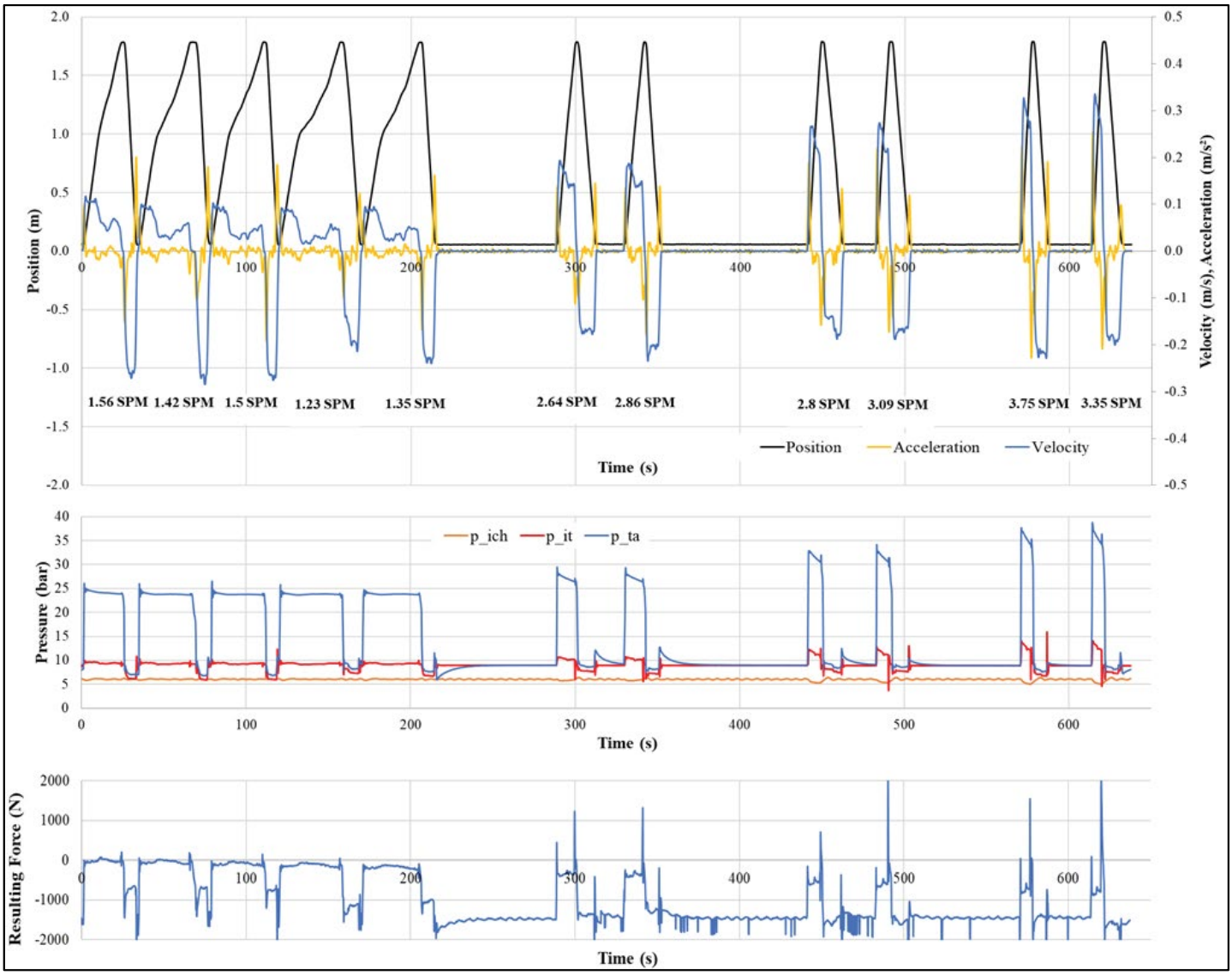

Figure 18: Test case 1 results.

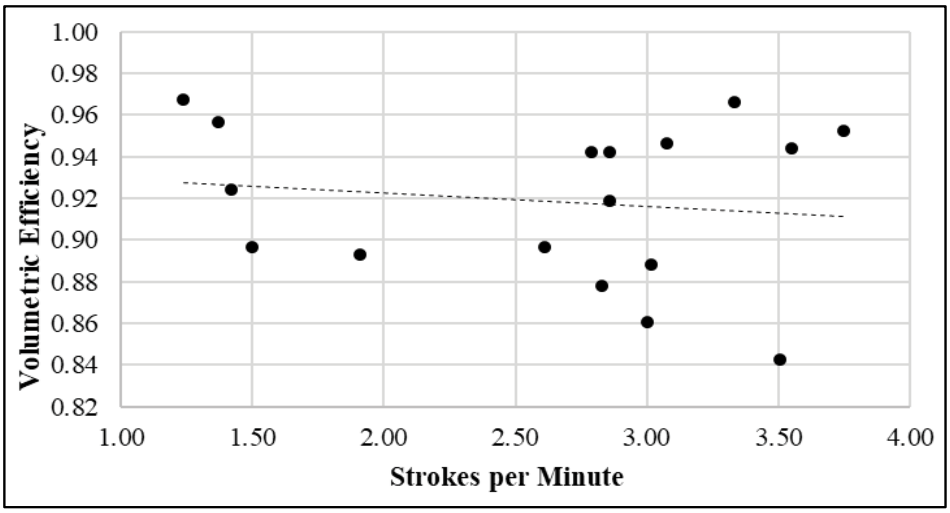

Figure 19: Volumetric pump efficiencies test case 1 to 3.

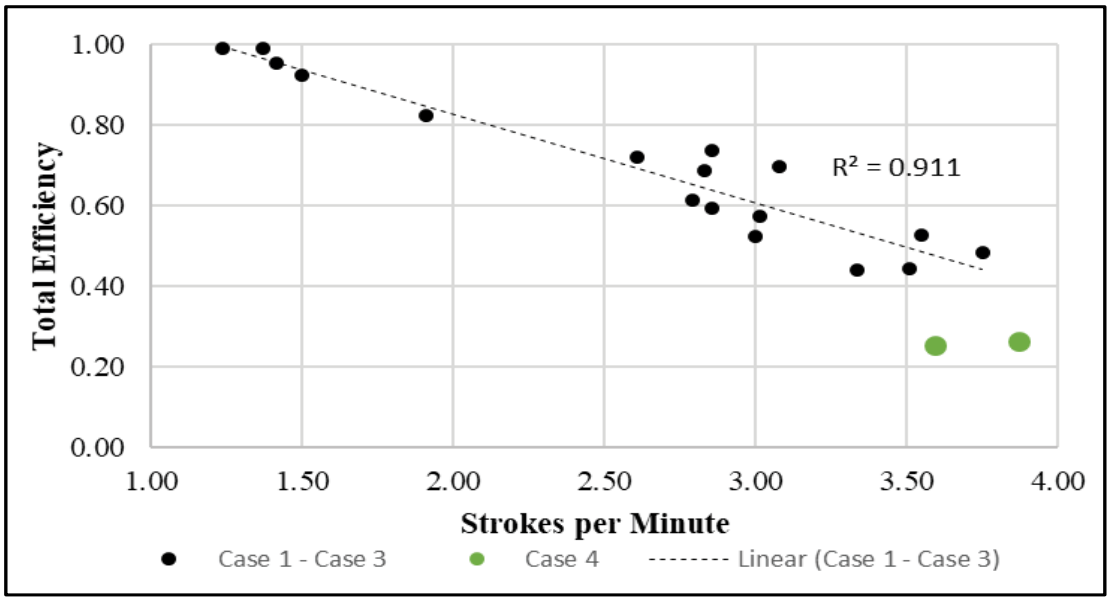

Figure 20: Total pump efficiencies.

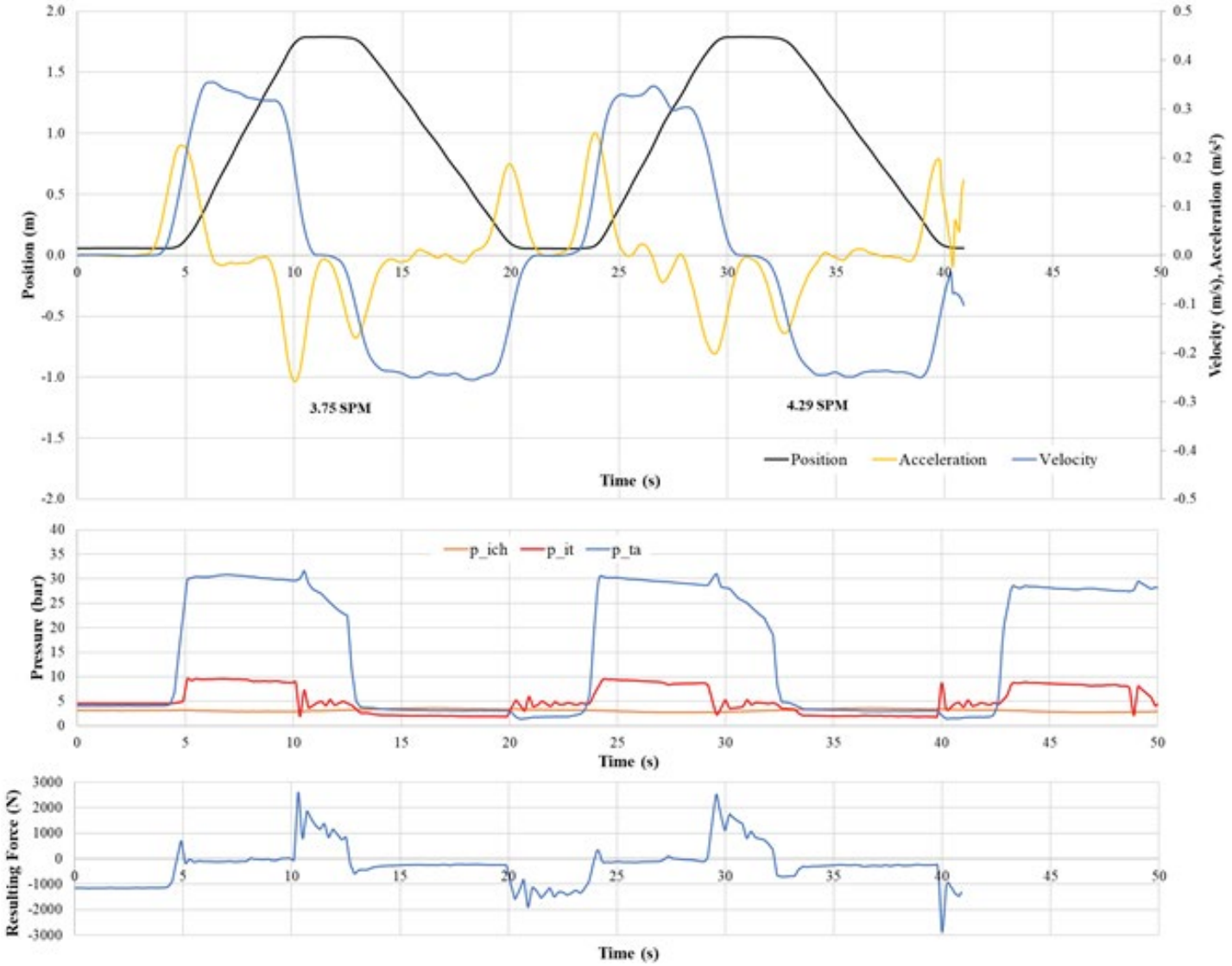

Figure 21: Test Case 4 results.

the reservoir pressure is 6 bar. The system's static equilibrium is reached at an injection pressure of 17.5 bar, which has been seen during the tests. The simulation confirms the speed of 1.5 SPM and the production rate of 9.4 m^3/day at a lift efficiency of 95.4 percent (Figure 21).

CONCLUSION

The hydraulic pump provides various advantages compared to other artificial lift systems for pumping geothermal fluid, unloading gas wells, and pumping heavy oil. There is no mechanical connection from the downhole pump to the surface, no over- and under-traveling of the plunger assembly, and the application can be used in any kind of wellbore inclination. The installation of the downhole pump can be done by wireline or by circulation. The upper pump plunger can be equipped with a check valve to inject inhibitors against corrosion and scaling. The liquid can quickly dilute heavy oil, injected through this check valve for improving the lifting properties. The power fluid injection rate depends on the plunger cross-section ratio but is typically lower than 40 percent, resulting in a small surface footprint compared to standard hydraulic pumping systems and improving the profitability for wells close to the economic limit. Various operation modes allow a high degree of flexibility, and the pumping system can be adjusted for various applications. Low to moderate production rates can be achieved.

The simulation model itself can be parameterized to control the simulation or change in basic geometry. The simulation has shown that the liquid level regulation is significant for the pumping operation. The unique working principle requires the power fluid columns to be alternating reciprocate during up- and downstroke. Nevertheless, high total efficiencies can be reached.

REFERENCES

1. Lea JF, Nickens HV, Wells MR. Gas well deliquification, (2nd edn). Burlington, Massachusetts, USA: Gulf Professional Publishing, 2008.
2. Turner RG, Hubbard MG, Dukler AE. Analysis and prediction of minimum flow rate for the continuous removal of liquids from gas wells. J Pet Technol. 1969; 21: 1475–1482.
3. Coleman SB, Clay HB, McCurdy DG. A New Look at Predicting Gas-Well Load-Up. J Pet Technol. 1991; 43: 329–333.
4. Romer MC, Brown M, Ainsworth N, Rundberg O, Bolt DJ, Bolt T, et al. Field trial of a novel self-reciprocating hydraulic pump for deliquification, SPE Prod & Oper. 2017; 32: 527–538.
5. Casey D. Guidelines & Recommended Practices. Selection of Artificial Lift Systems for Deliquifying Gas Wells. Soap Sticks, Prepared by Artificial Lift R&D Council, 2015.
6. Jain S, Al Hamadi MA, Jaber S, Jany AB. Mature Field Revitalization: Analysis of Wellhead Compression to Enhance Productivity from a Mature Retrograde Reservoir. Paper presented at the SPE/IATMI Asia Pacific Oil & Gas Conference and Exhibition, Nusa Dua, Bali, Indonesia, 2015.
7. Fadairo A, Adeyemi G, Ogunkunle T, Lawal O, Olugbenga O. Modelling minimum flow rate required for unloading liquid in gas wells. Paper presented at the SPE Nigeria Annual International Conference and Exhibition, Virtual, 2020.
8. Lake LW, Clegg JD. Petroleum Engineering Handbook, Volume 4, SPE, Richardson, Texas, USA, 2006.
9. Furrow B, Newman K, Bolt, DJ. Selection & Validation of Hydraulic Dewatering Pumps in the Natural Gas Industry: An Update. Presented at the ALRDC Gas Well Deliquification Workshop, Denver, 2012.
10. Brown KE. The Technology of Artificial Lift Methods, first edition. Tulsa: Pennwell Publishing Company, USA, 1980.
11. Fretwell J. Hydraulic Pumping in Oil Wells. In Petroleum Engineering Handbook, Volume IV: Production Operations Engineering, ed. J. D. Clegg and L. W. Lake, Chap. 2007; 14: 713–756.
12. Pugh T. Overview of hydraulic pumping (Jet and Piston). Report, Weatherford: Houston, Texas, USA, 2006.
13. Cenk T, Celal Hakan C, Minh T, Elsayed A, Bao J, Dike P, et al. A Comprehensive Review Heavy Oil Reservoirs, Latest Techniques, Discoveries, Technologies and Applications in the Oil and Gas Industry. Paper presented at the SPE International Heavy Oil Conference and Exhibition, Kuwait City, Kuwait, 2018.
14. Taheri A, Hooshmandkoochi A. Optimum Selection of Artificial Lift System for Iranian Heavy Oil Fields, Paper presented at the SPE Western Regional/AAPG Pacific Section/GSA Cordilleran Section Joint Meeting, Anchorage, Alaska, USA, 2006.
15. Brook G, Kantzas A. Evaluation of Non-thermal EOR Techniques For Heavy Oil Production. Presented at the Annual Technical Meeting, Calgary, Alberta, 1998.
16. Nasehi Araghi M, Asghari K. Use of CO_2 in Heavy-Oil Waterflooding, Presented at the SPE International Conference on CO_2 Capture, Storage, and Utilization, New Orleans, Louisiana, USA, 2010.
17. Butler RM, Mokrys IJ. A New Process (VAPEX) For Recovering Heavy Oils Using Hot Water And Hydrocarbon Vapour. J Canadian Petrol Technol. 1991; 30: 1.
18. Cavender T. Summary of Multilateral Completion Strategies Used in Heavy Oil Field Development. Presented at the SPE International Thermal Operations and Heavy Oil Symposium and Western Regional Meeting, Bakersfield, California, USA, 2004.
19. Worth D, Al-Safran E, Choudhuri A, Al-Jasmi A. "Assessment of Artificial Lift Methods for a Heavy Oil Field in Kuwait." Paper presented at the SPE International Heavy Oil Conference and Exhibition, Mangaf, Kuwait, 2014.
20. Mesbah H, Aarti D, Tanasescu I. Hybrid Artificial Lift System-Alternate SRP/PCP in Cyclic Steam Injection for Heavy Oil Wells, Paper presented at the SPE Middle East Artificial Lift Conference and Exhibition, Manama, Bahrain, 2018.
21. El Gharbawi MA, Elgibaly AA, Salem AM, Mohamed A. Performance Analysis of the Artificial Lift Systems for Heavy Oil Wells in the Egyptian Eastern Desert, Paper presented at the SPE Annual Technical Conference and Exhibition, Calgary, Alberta, Canada, 2019.
22. López Manríquez A, López Hernández JG. Using a New Hybrid Artificial Lift System for Mature Heavy Oil Fields, Paper presented at the SPE Heavy Oil Conference Canada, Calgary, Alberta, Canada, 2012.
23. Mata H, Aristizabal K, Rincon G, Duran JA, Pinto F. "Successful Installation of a Dual Concentric Completion System on 9 5/8" Casing ESP-ESP Type in Colombia." Paper presented at the SPE Artificial Lift Conference-Americas, Cartagena, Colombia, 2013.
24. Clegg JD. Petroleum Engineering Handbook Volume IV, Production Operations Engineering. 2007; p. 714.
25. Hofstätter H. Pump System, Patent number WO2011069517 A1, 2009.
26. Langbauer C, Vita P, Jax G, Hofstätter H. Hydraulic Concentric Tubular Pumping System for Unloading Gas Wells, SPE Asia Pacific Oil and Gas Conference, and Exhibition. Australia, 2018. [26]
27. American Petroleum Institute. API Specification 11AX – Specification for Subsurface Sucker Rod Pumps and Fittings, 2006.

28. Langbauer C, Hartl M, Gall S, Volker L, Decker C, Koller L, et al. Development and Efficiency Testing of Sucker Rod Pump Downhole Desanders, SPE Production & Operations, SPE-200478-PA, 2020.

29. Wilson P, Chilingarian GV. Chapter 15 - Hydraulic Subsurface Pumps, Developments in Petroleum Science, Elsevier. 1987; 19 (A): 635-736.

30. Flowguad USA. Pulsation Dampeners, 2016.

31. http:/openfoam.org/2021.

32. Jasak H, Tukovic Z. Automatic mesh motion for unstructured finite volume method, Transactions of FAMENA. 2007; 30: 1–18.

33. Jasak H. Dynamic Mesh Handling in OpenFOAM, presented at the 47th AIAA Aerospace Sciences Meeting including the New Horizons Forum and Aerospace Exposition, Orlando, Florida, USA, 2009.

34. Gschaider BFW. "Swak4Foam Library", 2017.

35. Jasak H. Error Analysis and Estimation for the Finite Volume Method with Applications to Fluid Flows, Ph.D. Thesis, Imperial College of Science, Technology, and Medicine, London, 1996.

36. Menter FR. Two-equation eddy-viscosity turbulence models for engineering applications, AIAA. 1994; 32: 1598–1605.

37. Jax G. Numerical Study on a new Hydraulic Subsurface Pump, Master Thesis, Montanuniversität Leoben, 2018.

38. Langbauer C, Fazeli-Tehrani F. Pump test facility for research, testing, training, and teaching, Erdöl Erdgas Kohle Magazin, 2020: 35-42.

39. Langbauer C, Fruhwirth RK, Lukas V. Sucker rod anti-buckling system-development and field application, SPE Production & Operations, 2021.